A Physics-motivated DNN for X-ray CT Scatter Correction

Berk Iskender and *Yoram Bresler*
Coordinated Science Laboratory and Department of ECE
University of Illinois, Urbana-Champaign

IEEE ISBI 2020

Introduction: X-ray CT

- X-ray CT imaging is based on materials absorbing photons according to their electron density

Measurements from different angles → *Computer processing* → Cross-sectional (tomographic) images

- Used widely for imaging internal structures of the body and non-destructive evaluation [1]

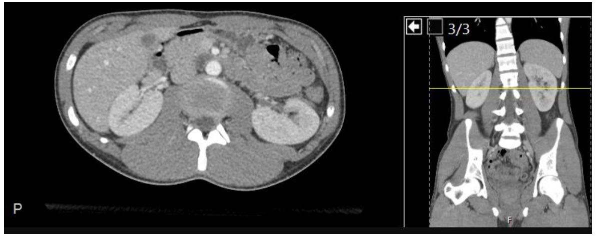

Abdomen and pelvis scan

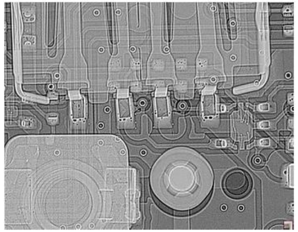

An electronic board

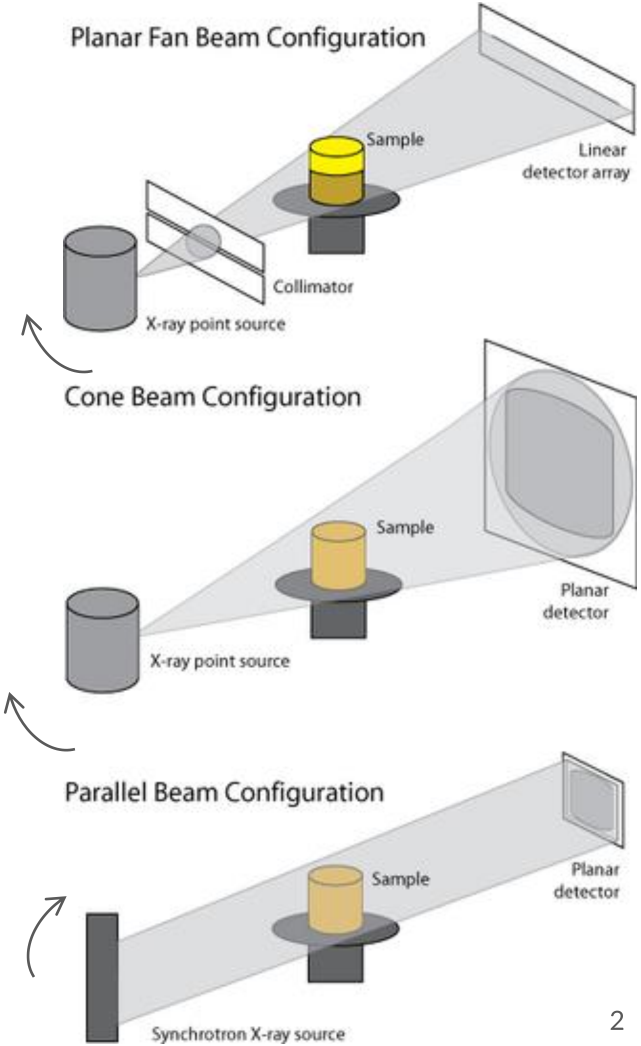

Problem: X-ray Scattering

- Additive contribution of scattered X-rays to measured signal causes artifacts

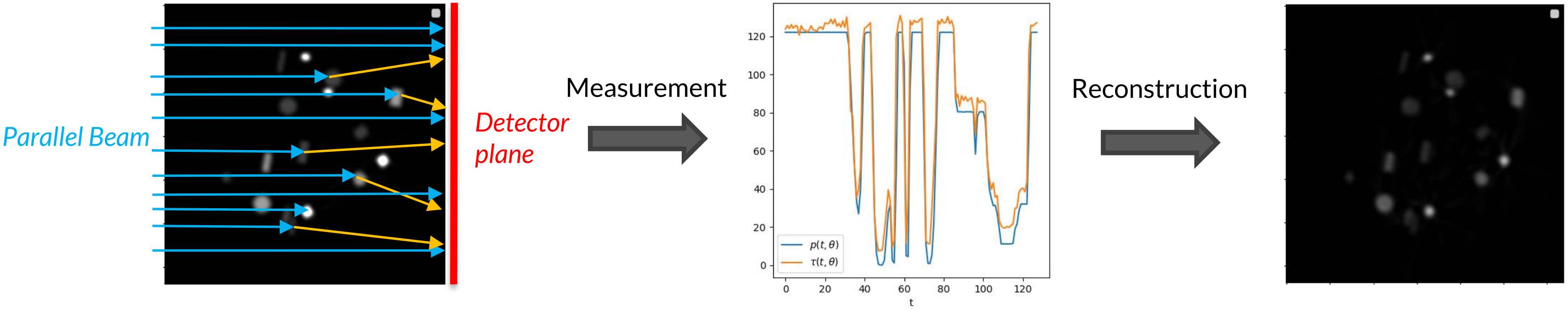

- **Reconstruction degradations** → streaks, cupping, shading artifacts and decreased contrast

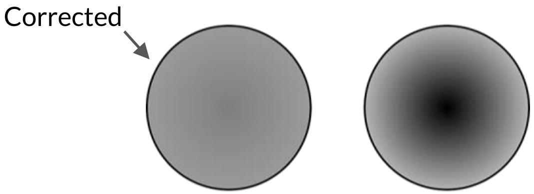

Cupping artifact

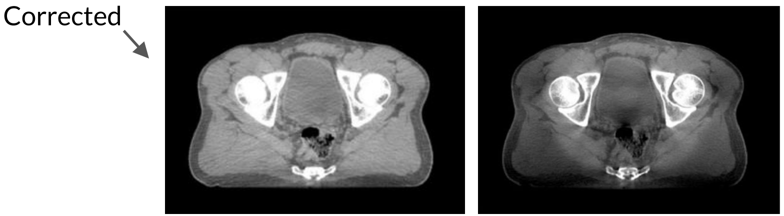

Shading artifact & decrease in contrast

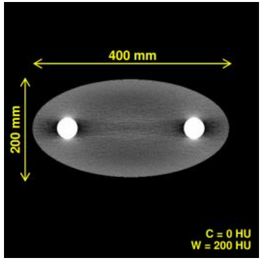

Streaking artifact

Problem Statement

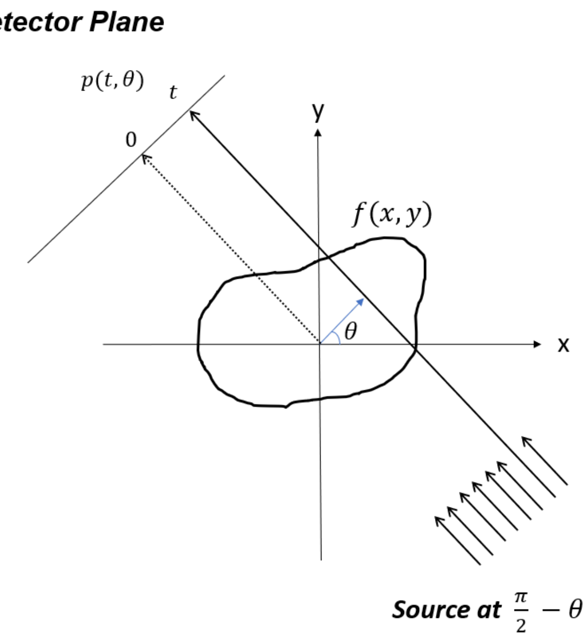

- In a 2D monochromatic parallel beam source setting at energy E_0, the **primary measurement** and **line integral projection** at angle $\theta \in [0, 2\pi)$ and position $t \in \mathbb{R}^d$

$$p(t,\theta) = I_0 e^{-g(t,\theta)} \qquad\qquad g(t,\theta) = (Rf)(t,\theta)$$

I_0: vacuum (air) measurement, $f(\boldsymbol{x})$: object, $x \in \mathbb{R}^2$, R: 2D Radon transform

- **Assumption: Beer's Law**

Photons lost by $\underbrace{\text{interaction}}_{\text{Compton sc., Rayleigh sc., photoelectric effect}}$ as attenuation on a straight-line path

- **Reconstruction:** $p(t,\theta) = I_0 e^{-g(t,\theta)} \rightarrow g(t,\theta) = -\ln \frac{p(t,\theta)}{I_0} \rightarrow f(\boldsymbol{x}) = (R^{-1}g)(\boldsymbol{x})$

R^{-1}: FBP algorithm

Problem Statement

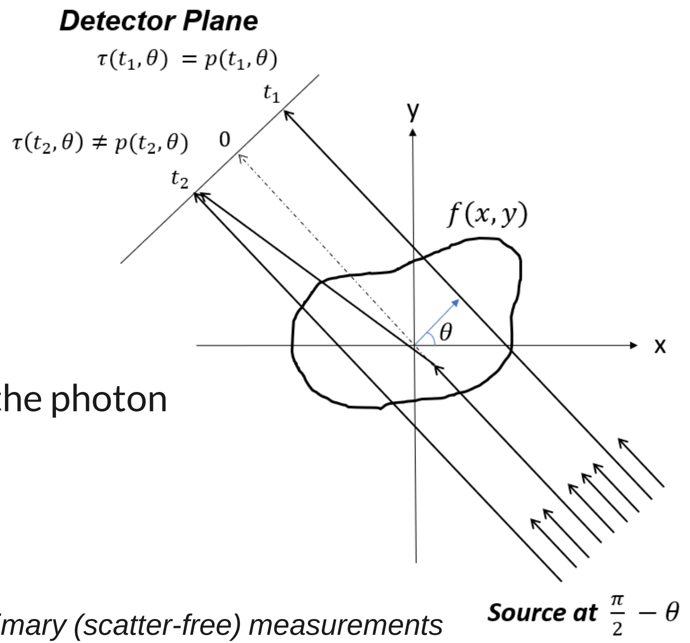

$$p(t,\theta) = I_0 e^{-g(t,\theta)} \qquad g(t,\theta) = (Rf)(t,\theta)$$

- **Reality:** Scattering causes a <u>change in the direction</u> (and energy) of the photon

$$\tau(t,\theta) = p(t,\theta) + s(t,\theta), \qquad s(t,\theta) \geq 0$$

$\tau \triangleq \{\tau_\theta, \theta \in \Theta\}$: *Set of total (scatter corrupted) measurements,* $p \triangleq \{p_\theta, \theta \in \Theta\}$: *Set of primary (scatter-free) measurements*

$s \triangleq \{s_\theta, \theta \in \Theta\}$: *Scatter term* ***(nonlinear function of f)***

- **Reconstruction:** $\tilde{g}(t,\theta) = -\ln\frac{\tau(t,\theta)}{I_0} \rightarrow \tilde{f}(\boldsymbol{x}) = (R^{-1}\,\tilde{g})(\boldsymbol{x})$

I_0: *vacuum (air) measurement ,* R^{-1}: *FBP algorithm*

Degradations

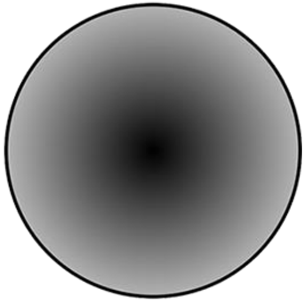

Cupping artifact

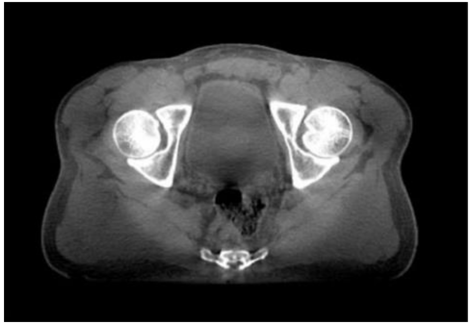

Shading artifact & decrease in contrast

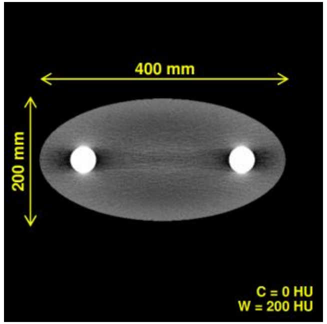

Streaking artifact

Scatter Correction Methods

Hardware-based

- Anti-scatter grids, collimators, primary modulation grids, etc.
- **Pros:** Successful in specific settings
- **Cons:**

1. Require modification of hardware
2. increase in scan time
3. Increase in dose

Software-based

1. Scatter estimation from the object:

   - Monte-Carlo (MC)-based scatter estimation

   - Analytical-numerical methods

2. Scatter estimation in projection domain

   - Kernel-based

   - Data-driven scatter estimation

Scatter Correction Methods

Hardware-based

- Anti-scatter grids, collimators, primary modulation grids, etc.
- **Pros:** Successful in specific settings
- **Cons:**

1. Require modification of hardware
2. increase in scan time
3. Increase in dose

Software-based

1. Scatter estimation from the object:

   - Monte-Carlo (MC)-based scatter estimation

   - Analytical-numerical methods

2. Scatter estimation in projection domain

   - Kernel-based

   - Data-driven scatter estimation

3. **Proposed method**: Data-driven scatter estimation from ***combined*** projection & object

Iterative Scheme

- Assumption: Given the object f, can compute the scatter estimate $s^* = \phi(f)$
  - Different methods use different $\phi(.)$

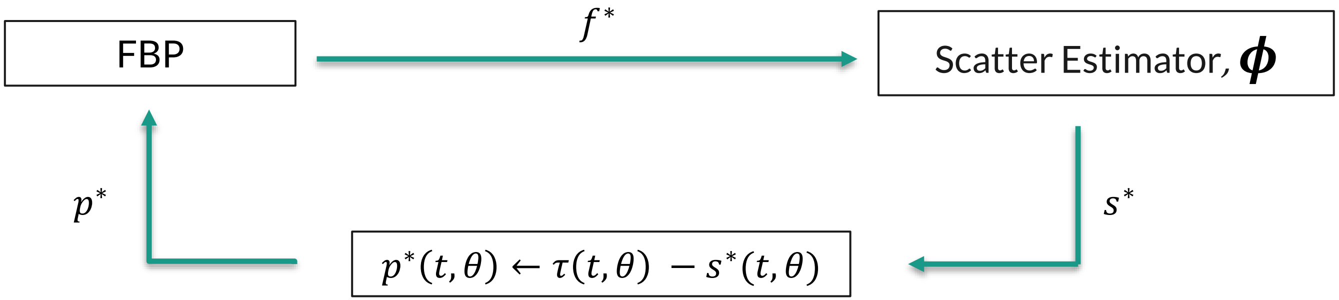

$\phi(.)'s$: Scatter Estimators from Given Object

MC based scatter correction (Poludniowski *et al* 2009):

- Stochastically sample photon propagation
- High computational cost and run times for clinical purposes

Trade-off: stochastic noise $\times$ run time

Deterministic linear Boltzmann transport equation (LBTE) solver: (Acuros, Maslowski *et al* 2018)

- Iteratively obtains an approximate solution of LBTE
- Faster than MC methods

Trade-off: accuracy $\times$ (discretization , # of iterations)

Slice-by-slice approach:

- First-order Compton scatter is modeled by distance-dependent blurring kernels (Bai *et al* 2000)
- Scatter is represented by convolutions applied to slices vertical to the photon propagation

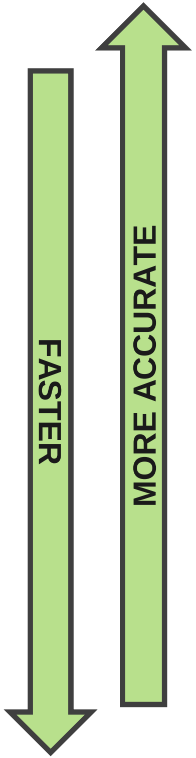

Kernel-based & Data-driven methods

Kernel-based methods:

- Estimate $s(t,\theta)$ using convolution of weighted $\tau(t,\theta)$ or an initial primary estimate with specific kernels (Ohnesorge et. al 1999)

$$s^*(t,\theta) = \tilde{\tau}(t,\theta) * G(t,\theta)$$

- Computationally efficient
- **Cons:** Prior assumptions and pre-defined kernels

G: kernel, *$\tilde{\tau}(t,\theta)$: weighted $\tau(t,\theta)$*

$$\tilde{\tau}_\theta \longrightarrow \boxed{G} \longrightarrow s_\theta^*$$

Block diagram for Kernel-based methods

Data-driven methods:

- Deep scatter estimation (DSE) (Maier et. al 2018)
- Estimate s_θ using DCNNs: $s_\theta^* = N(\tau_\theta)$
- **Cons:** scatter in one projection depends on entire object
  → cannot be determined from data in one view

  Loss function includes p_θ rather than g_θ

$$\tau_\theta \longrightarrow \boxed{N_\gamma()} \longrightarrow s_\theta^*$$

Block diagram for DSE

Proposed Method

- A new physics-motivated, deep learning-based method to estimate and correct scatter in projection measurements

- **New features: i)** Incorporates both an initial reconstruction $\tilde{f}_\theta$ and scatter-corrupted measurements τ_θ

  ⇒ Scatter estimate for each view angle θ depends on the entire object

  ii) Physics-motivated constraints

  iii) A specific DCNN

  iv) A specific cost function for training

- Operates on normalized quantities, $\bar{\tau}_\theta = \tau_\theta / I_0, \bar{p}_\theta = p_\theta / I_0, \bar{s}_\theta = s_\theta / I_0$ ⟶ applicability for various I_0

Block Diagram & Loss Function

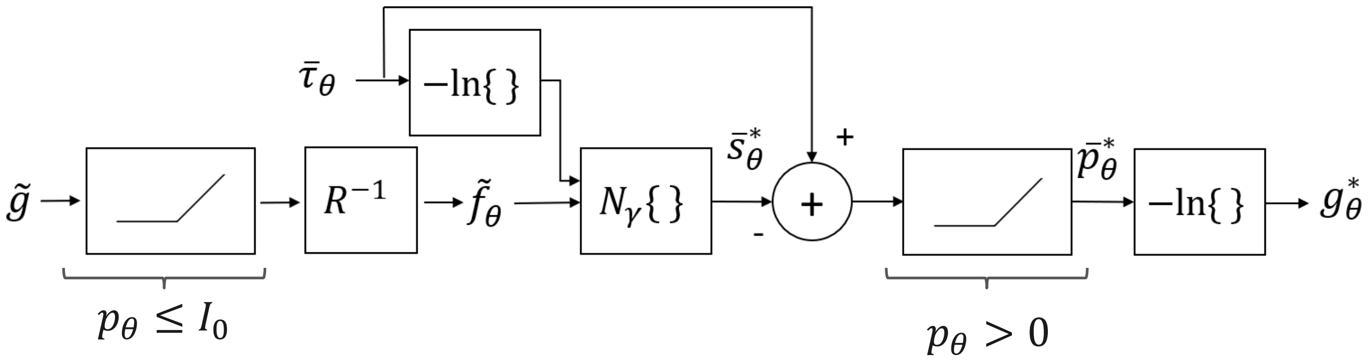

- After processing all views,

$$f^*(\boldsymbol{x}) = (R^{-1}g^*)(\boldsymbol{x})$$

- Loss function, L, for training the network,

$$L(g_\theta, g_\theta^*) = \min_\gamma \|h * (g_\theta - g_\theta^*)\|_2^2 + \lambda\|g_\theta - g_\theta^*\|_1$$

- $h[n] = \frac{1}{2}\delta[n+1] - \frac{1}{2}\delta[n-1],\ \lambda > 0$
- L is tailored to minimize errors in the reconstructed image, $f^*(\boldsymbol{x})$

(1) Particular h selection

(2) Post-log quantities g are used rather than p

Filter h

- Enables to express the norm of **an image-domain error** in **the projection domain** $\longrightarrow$ **No need for FBP in L**
  ($||Qf||_2$ in terms of g_θ, Q: a radially symmetric filter)
- Edges are perceptually significant $\longrightarrow$ Q is HPF
- Using Parseval's identity & projection-slice theorem $\longrightarrow$ $\boxed{\|Qf\|_2^2 = \|h * g\|_2^2}$
- Using Shepp-Logan filter in FBP and $Q(\nu) = |\nu|^{0.5}$ $\longrightarrow$ *(Short time-domain filter implementation)*

$$\boxed{h[n] = \frac{1}{2}\delta[n+1] - \frac{1}{2}\delta[n-1]}$$

DCNN, N_γ

- Operates view-by-view
- Inputs:
  1. A normalized post-log total measurement at view angle θ: $-\ln \bar{\tau}_\theta \in \mathbb{R}^d$
  2. Initial reconstruction estimate, rotated by θ: $\tilde{f}_\theta \in \mathbb{R}^{d^2}$
- Output:
  1. Normalized scatter component estimate: $\bar{s}^*_\theta \in \mathbb{R}^d$

$$\bar{s}^*_\theta = N_\gamma(\tilde{f}_\theta, -\ln \bar{\tau}_\theta)$$

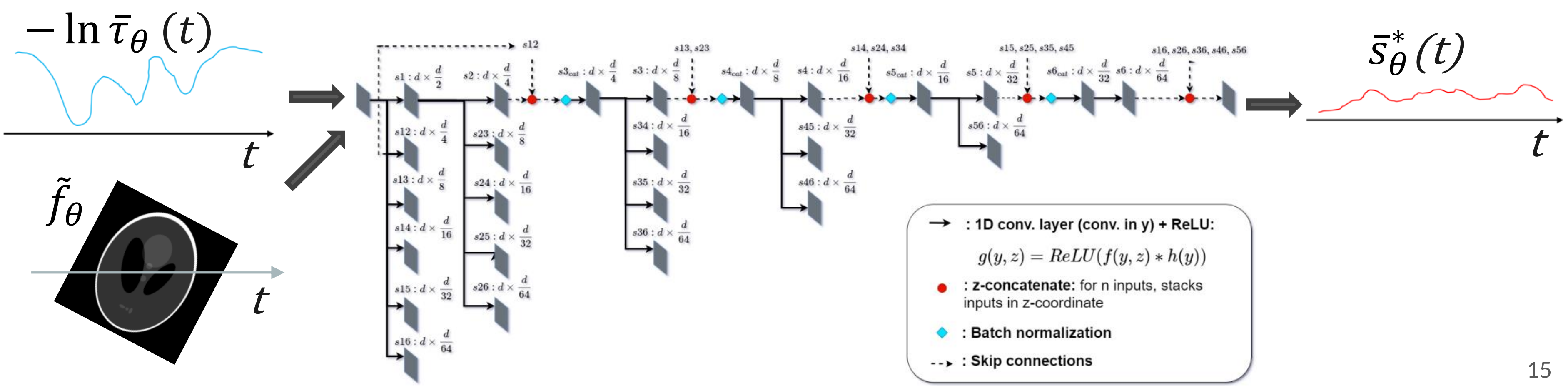

Data Generation, Training & Experiments

- $\boldsymbol{\tau_{\theta}}$: GATE – encapsulating GEANT4 MC simulation libraries.
- $K = 360$ views, each having $P = 2(10^6)$ photons
- $\boldsymbol{p_{\theta}}$: Using Beer's Law, $p(t, \theta) = I_0 e^{-(Rf_{E_0})(t,\theta)}$

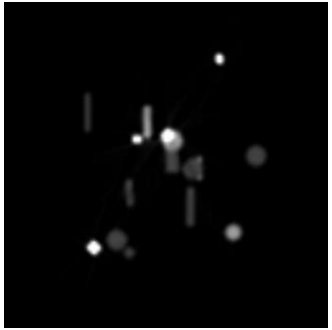

Training & Experiments:

- Data is divided into training and validation sets phantom-wise, all measurements of a phantom in the same set, 27 randomly synthesized phantoms
- 200 keV parallel beam setting
- Water, Al & steel objects
- Improvement over the 1D adapted DSE method in numerical experiments

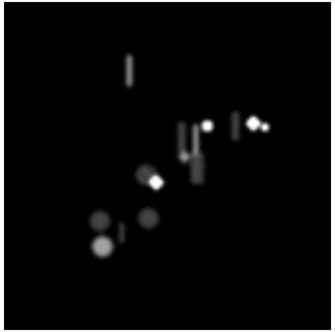

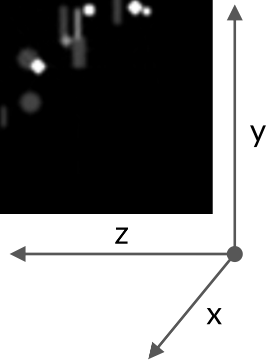

Computational Cost & Run times

- Total cost $< 3LKd^3$, dominated by DCNN

L: length of the filters in DCNN, d: size of measurements

- $K = 360$ views on GPU → **<u>only 4 ms</u>**

Results

f

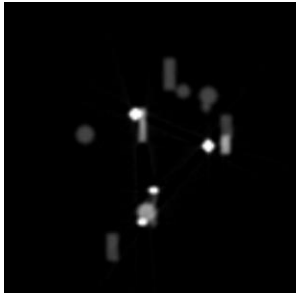

f using primary meas. p_θ

	Uncorr.	DSE-1D	Proposed
PSNR	31.39	37.90	**40.83**
SSIM	0.94	0.94	**0.97**
MAE	39.71	31.06	**17.85**

Table: Average reconstruction accuracies

Total meas. τ_θ

DSE-1D p^*_θ

Proposed method p^*_θ

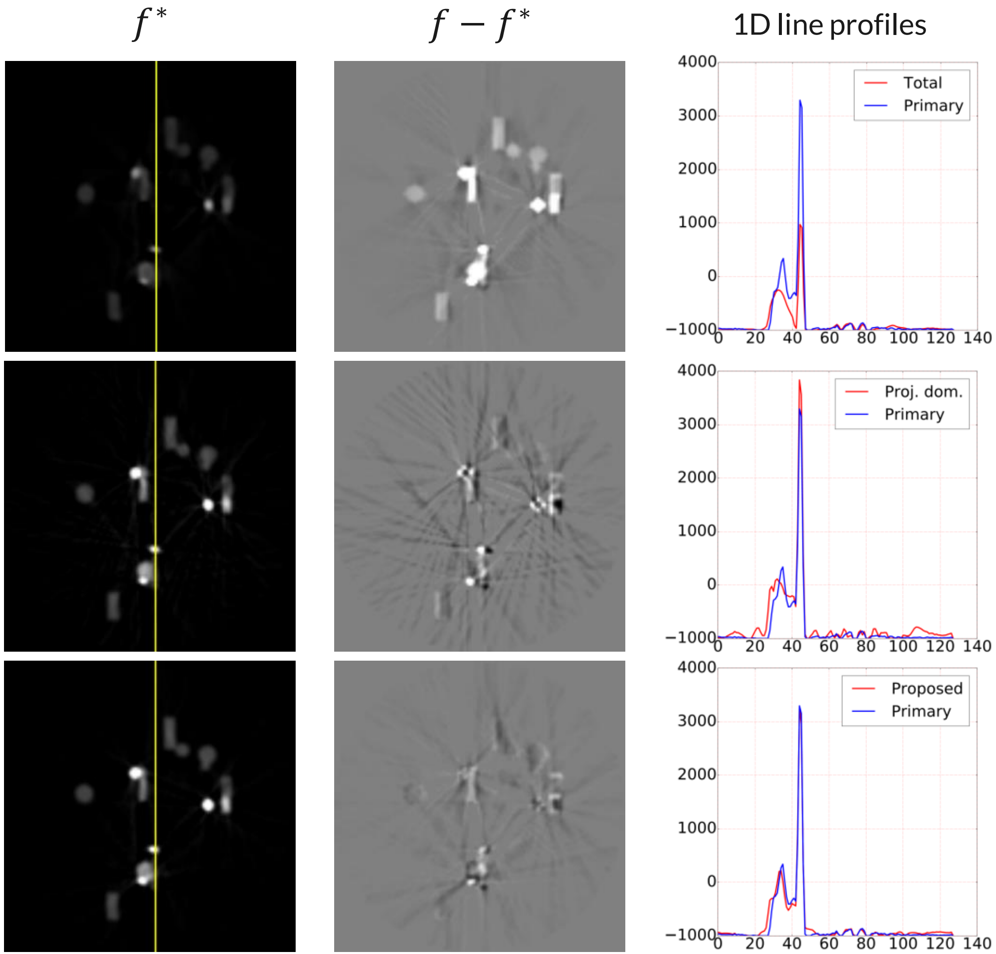

Conclusions

- Scattering in X-ray CT produces various degradations in the reconstructions
- A data-driven approach with physics-motivated constraints

  specific DCNN architecture

  specific cost function

Future Work

- Implementing the method for other CT geometries
- Extending the experiments for polychromatic beam setting & 3D reconstructions

References

1. Floyd C E, Jaszczak R J, Harris C C and Coleman R E 1984 Energy and spatial distribution of multiple order Compton scatter in SPECT: a Monte Carlo investigation *Phys. Med. Biol.* **29** 1217-30
2. H. E. Johns and J. R. Cunningham, *The physics of Radiology*, *Third edition* (Thomas, Springfield, Illinois, 1971), p. 167.
3. Poludniowski, G., et al. "An efficient Monte Carlo-based algorithm for scatter correction in keV cone-beam CT." *Physics in Medicine & Biology* 54.12 (2009): 3847.
4. C. Bai, G. L. Zeng, and G. T. Gullberg, “A slice-by-slice blurring model and kernel evaluation using the Klein Nishina formula for 3D scatter compensation in parallel and converging beam spect,” *Phys. Med. Biol.*, vol. 45, no. 5, 2000.
5. A. Maslowski et al., “Acuros CTS: A fast, linear Boltzmann transport equation solver for computed tomography scatter–Part I: Core algorithms and validation,”
   Med. Phys., vol. 45, no. 5, 2018
6. B Ohnesorge, T Flohr, and K Klingenbeck-Regn, “Efficient object scatter correction algorithm for third and fourth generation CT scanners,” *European radiology*, vol. 9, no. 3, 1999.
7. J. Maier et al., “Deep Scatter Estimation (DSE): Accurate real-time scatter estimation for X-ray CT using a deep convolutional neural network,” *Jour. of Nondest. Eval.*, vol. 37, no. 3, 2018.